

Effects of D₂O and Mixing on the Early Hydration Kinetics of Tricalcium Silicate

Jeffrey J. Thomas[†] and Hamlin M. Jennings^{*,†,‡}

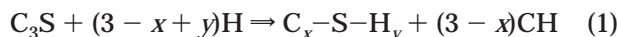
Departments of Civil Engineering and Materials Science and Engineering, Northwestern University, Evanston, Illinois 60208-3109

Received February 8, 1999. Revised Manuscript Received May 14, 1999

The hydration of tricalcium silicate powder with H₂O and D₂O was followed at three different temperatures using isothermal calorimetry. For both types of paste, the early kinetics could be accurately modeled, from the time of mixing to a point on the downslope of the main hydration peak, with a four-parameter nucleation and growth model. Pastes made with D₂O followed the same reaction path as pastes made with H₂O, with a reaction rate that was reduced by a factor of ~2.7 at a given temperature. The activation energy for hydration with D₂O is slightly higher than for H₂O. It is proposed that the slower reaction kinetics and higher activation energy in the presence of D₂O result from a kinetic isotope effect, whereby the increased mass of the hydrogen atom lowers the probability of the forward reaction at the atomic level.

Introduction

Tricalcium silicate (C₃S)^{1a} cement chemistry notation: C, CaO; S, SiO₂; H, H₂O; D, D₂O) is the primary component of portland cement and is responsible for most of the important properties of cement and concrete. The reaction between C₃S and water is complex, involving a series of sequential and parallel reaction steps, and the kinetics of this hydration reaction is not fully understood. The solid hydration products are the C–S–H gel and CH, and the reaction can be written as^{1b}



The formation of C–S–H and CH are linked by eq 1, and do not have independent kinetics. However, the ratio of CH to C–S–H does vary during the reaction, particularly at very early times. The C/S ratio of the C–S–H, which is variable x in eq 1, can vary from 1 to more than 2; a typical value for well-hydrated C₃S and portland cement is 1.7.² In saturated pastes, the H/S ratio of C–S–H, variable y in eq 1, is close to 4,² which includes the water-filled gel pores.

C₃S has an extremely high theoretical solubility, calculated at ~1 molal,³ and when C₃S and water are first combined there is a short period of fast reaction as the C₃S dissolves, lasting at most for a few minutes. This is followed by the well-known induction period, a period of perhaps 2 h during which almost no reaction occurs. The induction period is frequently attributed to the formation of a semipermeable layer around the C₃S

particles which acts as a diffusion barrier to dissolving ions. As discussed by Taylor et al.,⁴ there are a few different hypotheses regarding the precise nature of this layer and the cause of the end of the induction period.

During the next period of reaction, called the acceleratory period, the rate of reaction increases continuously, reaching a maximum at a time that is usually less than 24 h after initial mixing. Both the maximum reaction rate and the time at which it occurs depend strongly on the temperature and on the average particle size of the C₃S. The reaction rate then decreases rapidly to less than half of its maximum value, and then decreases much more slowly until all of the C₃S or all of the water is consumed, or all of the space available for reaction products is filled. This can take anywhere from a few days to years, again depending on the temperature and particle size. The kinetics and the different reaction stages associated with the hydration of C₃S are summarized in ref 5.

In this work, the hydration rate of C₃S pastes was measured using isothermal calorimetry at three different temperatures. The period of time during which the rate of nucleation and growth of C–S–H is rate controlling was then modeled using a standard Avrami approach which is described in the next section. This reaction stage encompasses the acceleratory period, starting when the reaction rate first begins to increase rapidly, and ends at some point during the deceleratory period, when diffusion of reactants to the reaction site becomes rate controlling.

In addition to temperature, the effects of initial mixing energy and the substitution of D₂O (heavy water) for H₂O on the early hydration kinetics of C₃S paste

[†] Department of Civil Engineering.

[‡] Department of Materials Science and Engineering.

(1) (a) Cement chemistry notation: C = CaO; S = SiO₂; H = H₂O; D = D₂O. (b) Tarrida, M.; Madon, M.; Rolland, B. L.; Columbet, P. *Adv. Cem. Based Mater.* **1995**, *2*, 15.

(2) Taylor, H. F. W. *Cement Chemistry*, 2nd ed.; Thomas Telford Ltd.: London, 1997.

(3) Stein, H. N. *Cem. Concr. Res.* **1972**, *2*, 167.

(4) Taylor, H. F. W. *Mater. Constr. (Paris)* **1985**, *17*, 457.

(5) Gartner, E. M.; Gaidas, J. M. In *Materials Science of Concrete*; Skalny, J. P., Ed.; American Ceramic Society: Westerville, OH, 1989; p 95.

were investigated. As first reported by King et al.,⁶ the hydration of C₃S and OPC with D₂O reduces the reaction rate by a factor of ~3. D₂O has a density that is 11% higher than H₂O, and most substances are less soluble in D₂O. However, D₂O and H₂O molecules are chemically very similar, and the exact reason for the lower hydration rate with D₂O has not yet been established. This issue is potentially quite important for the study of cement, since modern techniques such as NMR, neutron diffraction, and small-angle neutron scattering often use D₂O to increase signal strength and sensitivity or to enhance data analysis. In this paper, it is proposed that the change in kinetics is due to a reduction in the rate of chemical reaction between ions precipitating out of solution, a phenomenon known as a primary kinetic isotope effect.

The hydration of C₃S is a thermally activated process, and an activation energy is often calculated from the rate constants obtained at different temperatures. There is, however, a large scatter in reported activation energies in the literature. This issue is discussed in a separate section below.

Nucleation and Growth Kinetics

For any reaction with a rate controlled by a process of nucleation and growth, the kinetics can be modeled using an Avrami equation^{7,8} of the form

$$-\ln[1 - (\alpha - \alpha_0)] = [k(t - t_0)]^m \quad (2)$$

where α is the degree of reaction at time t , k is the rate constant, and m is an exponent. The constants α_0 and t_0 define the degree of reaction and time at which the nucleation and growth kinetic regime begins. Since the nucleation and growth regime begins along with the acceleratory period of hydration, α_0 is normally taken as zero, and eq 2 is thus a three-parameter model (m , k , and t_0). The time constant t_0 is nonzero, with a magnitude that corresponds loosely to the induction period.

When the rate of hydration is modeled as a function of time rather than as a function of degree of hydration, eq 2 can be differentiated, giving a related expression of the form

$$d\alpha/dt = Amk^m(t - t_0)^{m-1} \exp\{-[k(t - t_0)]^m\} \quad (3)$$

where a fourth parameter has been introduced: A , a preexponential factor. Equations 2 and 3 are sometimes used in a slightly different form with the parameter k appearing outside the square brackets in the exponential term [e.g., 8, 9]. In this case, k is not a true rate constant because it must take on units of time^{-m} for the exponential term to be unitless, and thus, unless m happens to be 1, it cannot be used to calculate an activation energy. If this parameter is called K , the relationship to the true rate constant k in eqs 2 and 3 is simply $k = K^{1/m}$.

The Avrami exponent m can be further defined in terms of three additional constants:^{7,8}

$$m = (P/S) + Q \quad (4)$$

where P is a dimensionality constant for the growth of product: $P = 1$ for 1D growth (fibers, needles, etc.); $P = 2$ for 2D growth (plates, sheets); and $P = 3$ for 3D growth (spheres, polygons). S is related to the rate-limiting growth mechanism: $S = 1$ for interface- or phase boundary-controlled growth, or $S = 2$ for diffusion-controlled growth. Q is a constant determined by the nucleation rate: $Q = 1$ for a constant nucleation rate, and $Q = 0$ for nucleation site saturation (zero nucleation rate).

The parameter k is a combined rate constant, including the rate constants for nucleation, for growth of product, and for other factors assumed to remain constant for a given kinetic process, such as diffusion coefficients.⁸ An apparent activation energy calculated using values of k obtained from eqs 2 or 3 therefore represents a sort of average temperature dependence for the independent nucleation and growth processes. Within a defined temperature range, such as the range of typical hydration temperatures of cements, this apparent activation energy is a useful way to describe the temperature dependence of the overall reaction rate, assuming that the rate-controlling step for the reaction does not change within the given temperature range.

Reported Activation Energies for Early C₃S Hydration

It has long been recognized that the kinetics of C₃S hydration can be divided into at least two major stages, an early fast reaction period, and a later period of diffusion-controlled reaction.¹⁰ The fast reaction period, which begins at the end of the induction period and continues past the maximum in the rate of heat evolution, has a significantly higher activation energy than the later diffusion-controlled kinetics. This is in good agreement with kinetic theory, which states that aqueous, diffusional-controlled processes have activation energies less than 20 kJ/mol, while processes controlled by rates of chemical reaction tend to have significantly higher activation energies.¹¹ This change in the activation energy during the hydration process has no doubt contributed to the perception that the activation energy for C₃S hydration is highly variable or difficult to measure.

Table 1 lists reported activation energies for C₃S hydration. Taplin¹² measured the degree of hydration by a loss-on-ignition method and obtained rate constants by assuming linear kinetics during the early reaction period, a rather extreme approximation. His activation energies range from 31 to 41 kJ/mol. Copeland and Kantro¹³ monitored the disappearance of alite in OPC

(9) FitzGerald, S. A.; Neumann, D. A.; Rush, J. J.; Bentz, D. P.; Livingston, R. A. *Chem. Mater.* **1998**, *10*, 397.

(10) Kondo, R.; Daimon, M. *J. Am. Ceram. Soc.* **1969**, *52*, 503.

(11) Laidler, K. J. *Chemical Kinetics*, 3rd ed.; Harper and Row: Cambridge, 1987.

(12) Taplin, J. H. *Proc. Int. Symp. Chem. Cem.* **1968**, *5*, Vol. 2, 337.

(13) Copeland, L. E.; Kantro, D. L. *Proc. Int. Symp. Chem. Cem.* **1968**, *5*, Vol. 2, 387.

(6) King, T. C.; Dobson, C. M.; Rodger, S. A. *J. Mater. Sci. Lett.* **1988**, *7*, 861.

(7) Avrami, M. *J. Chem. Phys.* **1939**, *7*, 1103; **1940**, *8*, 212.

(8) Brown, P. W.; Pommersheim, J.; Frohnsdorff, G. *Cem. Concr. Res.* **1985**, *15*, 35.

Table 1. Reported Activation Energies for the Early Hydration Kinetics of C₃S^a

authors	technique	activation energy (kJ/mol)
Taplin ¹²	loss on ignition	31–41
Copeland and Kanthro ¹³	X-ray diffraction	41
Copeland and Kanthro ¹³	isothermal calorimetry	38.9
Kondo and Daimon ¹⁰	isothermal calorimetry	(30–32)
Tenatousse and de Donder ¹⁴	isothermal calorimetry	33
Fuji and Kondo ¹⁵	free lime measurement	31.4
Fierens et al. ¹⁶	isothermal calorimetry	49–50
FitzGerald et al. ⁹	quasielastic neutron scattering	(36.8)

^a Values in parentheses are recalculated values based on the original kinetic data, as justified in the text.

paste using quantitative X-ray diffraction, and report a value of 41 kJ/mol based on the rate of reaction at the relatively advanced degree of hydration of 60%. They claimed that the hydration of alite had not entered diffusion control even at that late stage. The same authors¹³ also measured the hydration of pure C₃S using isothermal calorimetry and obtained a value of 38.9 kJ/mol from data taken much earlier in the reaction.

Kondo and Daimon¹⁰ made an important contribution in 1969, when they proposed five different stages for the reaction, including the induction period. They defined the acceleration period, which they correctly attributed to nucleation and growth, as ending at the maximum in the rate of heat evolution, which is not necessarily the case. They report three apparent activation energies for the acceleratory period: 54, 100, and 155 kJ/mol, and these values have been cited by other researchers as indicative of a highly variable activation energy. However, the values of 100 and 155 kJ/mol were not obtained from rate constants, which by definition have a time dependence of time⁻¹, but rather from second and third derivatives of the reaction rate with time units of time⁻² and time⁻³, respectively. These parameters can be converted to effective rate constants by raising them to 1/2 and 1/3 powers, a process, which results in activation energies of 50 and 51.7 kJ/mol. Further confusing the issue, the Arrhenius slopes were calculated incorrectly; the original kinetic data, as reported in ref 10, actually yields activation energies of 32, 30, and 31 kJ/mol.

Tenatousse and de Donder¹⁴ were the first to model the rate of hydration using the Avrami nucleation and growth equation (eq 3). Using isothermal calorimetry, they obtained an exponent value of $m = 3$ and calculated an activation energy of 33 kJ/mol. They also showed that the nucleation and growth kinetics extended past the maximum in the rate of hydration. The observation that the Avrami nucleation and growth equation accurately models the shape of the hydration rate peak is strong evidence in favor of a nucleation and growth process.

Fuji and Kondo¹⁵ measured the degree of hydration by monitoring the amount of free lime, and analyzed the kinetics using a different nucleation and growth equation, obtaining an activation energy of 31.4 kJ/mol. Fierens et al.¹⁶ used the Avrami equation to model the early kinetics, assuming a fixed value of 3 for the

exponent on the basis of the work of Tenatousse and de Donder.¹⁴ From isothermal calorimetry, they obtained activation energies of 49 and 50 kJ/mol for two different batches of C₃S.

FitzGerald et al.⁹ recently used quasielastic neutron scattering to measure the rate of hydration of C₃S pastes and were able to model the hydration rate using the Avrami nucleation and growth equation. They reported an activation energy of 31 kJ/mol. However, this value was not based on rate constants with units of time⁻¹ (see discussion in previous section). Reanalysis of their reported data yields a corrected activation energy value of 36.8 kJ/mol.

Reference to Table 1 shows that the majority of the reported activation energy values are between 30 and 41 kJ/mol, with the sole exception being the higher values of Fierens et al.¹⁶ This is not an unreasonable range, considering that different experimental methods have been used to measure the rate or degree of hydration and that different methods of calculating or estimating rate constants have been used. It should also be noted that there are wide variations in the reactivity of C₃S powder, and that different polymorphs of C₃S behave differently.¹⁷ The activation energies reported in this work fall into the above range, and agree closely with the value of FitzGerald et al.,⁹ which was also calculated using an Avrami nucleation and growth model.

An important question regarding the early kinetics of C₃S hydration, which has remained unanswered, is the rate-controlling step. Possible rate-controlling steps in a nucleation and growth reaction include the rate of dissolution of ions into solution, the rate of diffusion of ions to the reaction site, and the rate of chemical reaction between ions to form the product phase. In this work, careful measurements of the rate of reaction of C₃S pastes made with H₂O and D₂O and hydrated under identical conditions were made. The goal was to identify specific differences in the reaction kinetics that could be used to determine the rate-controlling step for early C₃S hydration.

Experimental Section

All experiments were performed using a phase-pure monoclinic C₃S powder with a Blaine fineness of 3602 cm²/g (Construction Technology Laboratories, Skokie, IL). C₃S pastes were made by combining C₃S and either deionized H₂O or D₂O (Cambridge Isotope Laboratories, 99.9% pure). The water to solids ratio (w/s) for pastes made with H₂O was either 0.4 or 0.5. For pastes made with D₂O, the amount of D₂O was adjusted to give the equivalent volume of liquid as with an H₂O paste with $w/s = 0.4$, resulting in an actual w/s values of 0.44 (D₂O has a density of 1.11 g/cm³). Pastes were mixed inside the stainless steel holders designed for use in the calorimeter, which hold ~1 g of paste. The holder was then sealed and placed into the calorimeter (Differential Scanning Calorimeter, Hart Scientific, Pleasant Grove, UT) where it was maintained at a constant temperature. Temperatures of 20, 30, and 40 °C were used.

To test the effect of mixing on the early kinetics, C₃S/H₂O pastes made with w/s values of 0.4 or 0.5 were mixed in one of two ways. Some pastes were gently combined only until the C₃S was completely wet by the H₂O, giving the paste a uniform

(14) Tenatousse, N.; de Donder, A. *Silic. Ind.* **1970**, *35*, 301.

(15) Fujii, K.; Kondo, W. *J. Am. Ceram. Soc.* **1974**, *57*, 492.

(16) Fierens, P.; Kabuema, Y.; Tirloq, J. *Cem. Concr. Res.* **1982**, *12*, 191.

(17) Stewart, H. R.; Bailey, J. E. *J. Mater. Sci.* **1983**, *18*, 3686.

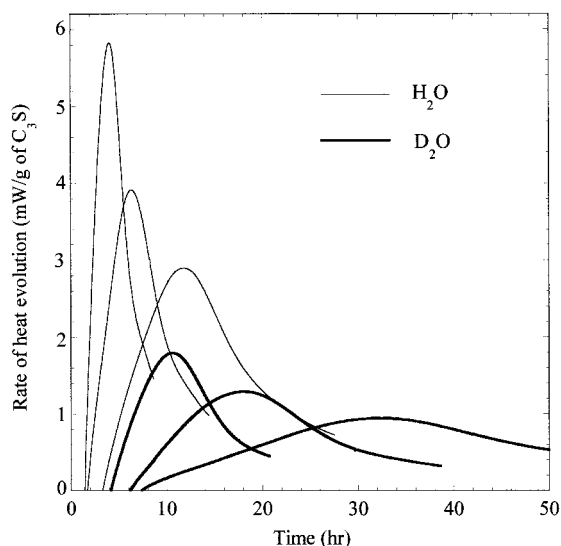


Figure 1. Isothermal calorimetry data for C_3S/H_2O and C_3S/D_2O pastes with $w/s = 0.4$, mixed for 5 min by hand. For each type of paste, the highest peaks are 40 °C and the lowest peaks are 20 °C; the intermediate peaks are 30 °C.

texture, a procedure which will be referred to for clarity as “no mixing.” Other pastes were vigorously hand-mixed with a small wire for 5 min. These specimens were hydrated isothermally at either 20, 30, or 40 °C in the calorimeter.

Results and Discussion

Effect of Initial Mixing on the Hydration Kinetics. Calorimetry data for C_3S/H_2O and C_3S/D_2O pastes hydrated at 20, 30, and 40 °C are shown in Figure 1. The large decrease in the kinetics associated with hydration in D_2O is in good agreement with published results,^{6,18} as is the effect of temperature on the kinetics.

Vigorous hand mixing of C_3S/H_2O pastes shortened the length of time to the maximum in the rate of heat evolution (t_{max}), and lowered the magnitude of the maximum rate (R_{max}), as compared to pastes which were only combined gently (no mixing). This was observed at all three temperatures and for pastes made with both H_2O and D_2O (see Table 2).

Dollimore and Mangabhai¹⁹ found that increased mixing decreased the time to the maximum in the heat evolution for a Portland cement/silica fume blend hydrated at 20 °C. However, they report an increase in the magnitude of R_{max} with increased mixing of the paste, in contrast with the current results. Somewhat surprisingly, no other data in the literature regarding the effect of mixing on the early kinetics were found.

The maximum in the rate of heat evolution, R_{max} , is plotted as a function of t_{max} for all the runs in Figure 2. It was found that the all the data for a given mixing condition (mixing or no mixing) could be fitted quite well using a simple power-law relationship of the form

$$R_{max} = C/t_{max}^n \quad (5)$$

where C and n are constants. Little difference was observed in C_3S/H_2O pastes made with w/s values of 0.4

Table 2. Kinetic Data for the All the Runs^a

T (°C)	paste liquid	mixing	R_{max} (mW/g)	t_{max} (h)	t_0 (h)	m	k (h ⁻¹)
20	H_2O	no mix	3.21	13.1	3.49	2.63	0.0822
20	H_2O	mixed	2.59	11.9	3.12	2.53	0.0933
20	D_2O	no mix	0.88	37.4	7.16	2.64	0.0273
20	D_2O	mixed	0.83	33.0	6.28	2.61	0.0309
30	H_2O	no mix	4.93	8.1	1.89	2.53	0.1321
30	H_2O	mixed	4.22	6.8	1.18	2.65	0.1497
30	D_2O	no mix	1.63	22.4	3.76	2.56	0.0460
30	D_2O	mixed	1.49	17.9	2.75	2.44	0.0519
40	H_2O	no mix	7.60	5.2	1.10	2.63	0.2070
40	H_2O	mixed	6.82	4.1	0.68	2.51	0.2421
40	D_2O	no mix	2.91	13.8	2.32	2.52	0.0742
40	D_2O	mixed	2.55	10.6	1.51	2.62	0.0870

^a R_{max} and t_{max} are the maximum rate of heat evolution and the time at which the maximum occurs, and are determined from the experimental data. The parameters t_0 , m , and k are from the Avrami fits to the data and are defined by eq 3.

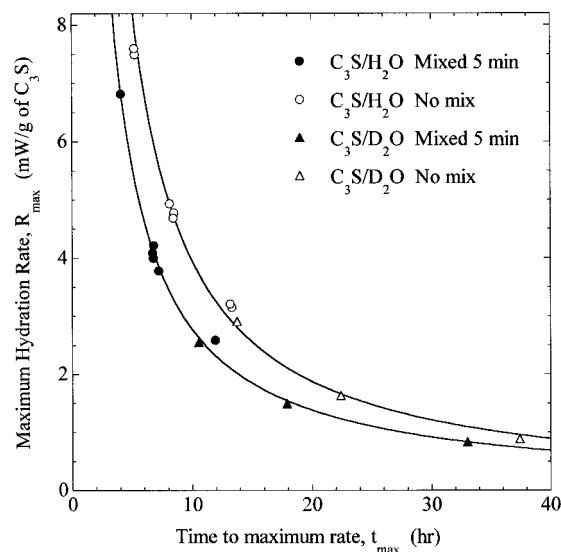


Figure 2. The maximum rate of heat evolution plotted against the corresponding time for the maximum, for different types of pastes (see legend). For a given data set, temperature decreases to the right from 40 to 20 °C. The lines are fits to the data according to eq 5; the fit parameters are given in Table 3.

Table 3. Fit Parameters and R^2 Values for the Data Fits Shown in Figure 2 for the Relationship between R_{max} and t_{max} Given by Eq 5

mixing procedure	C (mW/g)	n	R^2
no mixing	46.76	1.07	0.995
5-min mix	28.02	1.00	0.996

and 0.5, and these data were fitted together. The fits are shown in Figure 2. It is interesting to note that pastes made with H_2O and D_2O can be fitted to one rate equation.

The values of C and n from eq 5, along with the R^2 values of the fits, are given in Table 3. Initial mixing of the pastes was found to decrease the constant C , but the exponent n is close to 1 in both cases. It should be noted that there is no underlying physical basis for the form of eq 5. Several other types of fits such as logarithmic and exponential were also used to fit the data, but the quality of the fit was significantly worse in each case. The proximity of the n values to unity suggests a simple inverse proportionality between R_{max} and t_{max} .

(18) Thomas, J. J.; Jennings, H. M.; Allen, A. J. *Cem. Concr. Res.* **1998**, *28*, 231.

(19) Dollimore, D.; Mangabhai, R. J. *Thermochim. Acta* **1985**, *85*, 223.

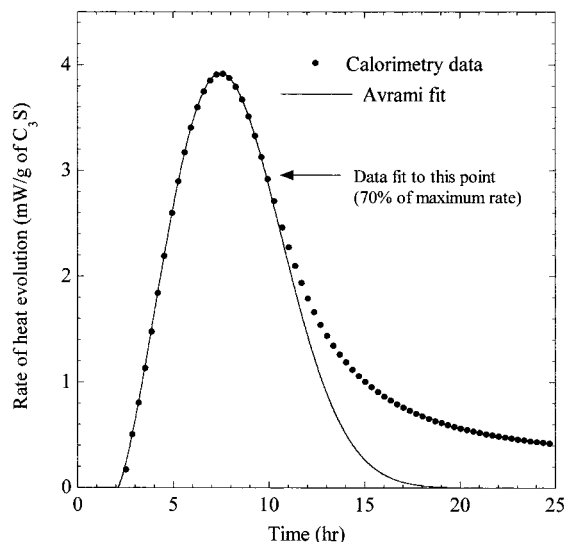


Figure 3. Calorimetry data for a C_3S/H_2O paste hydrated at $30^\circ C$, and the corresponding four-parameter Avrami fit. Only 5% of the calorimetry data is shown, to allow both data and fit to be seen.

Avrami Fits to the Kinetic Data. The data from each run were fit to the four-parameter Avrami equation relating rate of reaction to hydration time (eq 3). A nearly perfect fit could be achieved by fitting to the experimental data from the point when the hydration rate begins to accelerate rapidly to a point somewhere past the maximum in the rate of heat evolution. The point at which the experimental curve begins to deviate away from a fit to the earlier data was interpreted as the point when the rate of diffusion of reactants through the C–S–H product layer begins to control the hydration rate, and can be considered the true end of the nucleation and growth period. After some experimentation, the endpoint for the fit was chosen to be the point at which the hydration rate had fallen to 70% of its maximum value (R_{max}). An example of a fit to the kinetic data is shown in Figure 3.

The induction period t_0 , Avrami exponent m , and rate constant k are listed in Table 2 for all the runs. As expected, the rate constants at a given temperature are considerably lower for pastes reacted with D_2O , by a factor of 2.7 to 3. The induction periods are also longer for D_2O pastes, although by a somewhat smaller factor.

For a given temperature and paste liquid, mixing of the paste reduces the induction period and increases the rate constant. Both of these trends contribute to the significant decrease in the time to the maximum in the hydration rate, t_{max} , observed after mixing.

The rate constants listed in Table 2 were used to calculate activation energies for each type of paste. The rate constant is assumed to have a temperature dependence described by

$$k(T) = A \exp(-E_a/RT) \quad (6)$$

where k is the rate constant, E_a is the activation energy, T is the absolute temperature, and R is the gas constant. As shown in Figure 4, plots of $\ln(k)$ vs $1/T$ for the four types of C_3S pastes are all quite linear. The activation energies, calculated from the slopes of the plots in Figure 4, are listed in Table 4. The values fall within the range of previously reported values summarized in

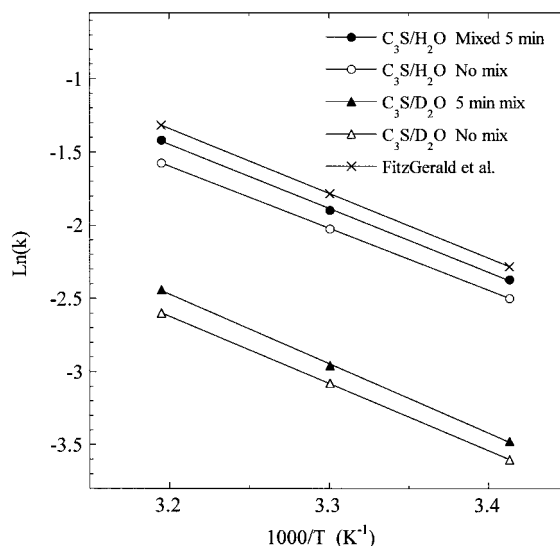


Figure 4. Avrami rate constants k , plotted as $\log(k)$ vs $1/T$ for various types of C_3S pastes (see legend). The slope of these plots is $-E_a/R$, as defined by eq 7. The activation energy values are listed in Table 4.

Table 4. Calculated Activation Energies for C_3S Pastes Made with H_2O and D_2O , with and without Initial Mixing

paste	E_a (kJ/mol)
C_3S/H_2O , no mix	35.2
C_3S/H_2O , 5-min mix	36.3
C_3S/D_2O , no mix	38.1
C_3S/D_2O , 5-min mix	39.4

Table 1. The activation energies are moderately higher for C_3S/D_2O pastes, and slightly higher for pastes that were vigorously hand-mixed, although the latter difference may be within experimental error.

Variation of the Avrami Exponent. The value of the Avrami exponent, m , is of considerable theoretical interest because it can be related to the type of nucleation and growth process taking place, including the morphology of the reaction product. The Avrami exponents from the fits to the data are listed in Table 2. They all fall within a range of 2.44–2.65, and there do not appear to be any trends related to mixing, temperature, or the use of H_2O and D_2O . Previous Avrami fits to C_3S hydration data obtained from calorimetry near room temperature have resulted in m values close to 3,^{15,16} in reasonable agreement with the current results.

The significance of the observed variation in m , and in variations in reported values of m from different techniques, depends to a large degree on how sensitive the quality of the four-parameter Avrami fits are to the value of m . This sensitivity was tested by fitting equations with different fixed values of m . For a given run, we found that if the value of m was fixed within a range of about $\pm 10\%$ of the best-fit value, a good fit to the data could still be obtained by optimizing the other three Avrami parameters (A , t_0 , and k). This procedure was necessarily rather subjective, but it gives a guideline for the magnitude of the variation in m which should be considered significant.

The variations in the value of m listed in Table 2 are within the nominal range over which good fits to an individual data set can be made. Therefore, we do not attribute any physical significance to the variation.

Table 5. Avrami Fit Parameters as Reported by FitzGerald et al.⁹ for the Hydration Rate of C₃S/H₂O Pastes As Measured by QENS

<i>T</i> (°C)	<i>t</i> _{max} ^a	<i>t</i> ₀ (h)	rate parameter (h ^{-<i>m</i>})	<i>m</i>	<i>k</i> (h ⁻¹) ^b
20	10.2	3.5	7.4 × 10 ⁻³	2.15	0.1021
30	5.7	1.5	1.74 × 10 ⁻²	2.27	0.1678
40	3.2	0.5	3.3 × 10 ⁻²	2.59	0.2679

^a Estimated from Figure 3 of ref 9. ^b *k* = (rate parameter)^{1/*m*}.

The effect of temperature on the Avrami exponent was first reported by Double et al.²⁰ for the early hydration of portland cement as measured by thermal calorimetry. They found that *m* increased with temperature, from 2.12 at 20 °C to 2.27 at 40 °C. Because the heat evolution of Portland cement has contributions from phases other than C₃S, their Avrami fits are significantly worse than achieved for pure C₃S in this work, and the observed increase in *m* with temperature is well within the range over which fits to cement hydration data could be made.

Brown et al.⁸ used the standard three-parameter Avrami equation (eq 2) to fit the quantitative X-ray diffraction (QXRD) data of Kondo and Daimon,¹⁰ resulting in *m* values close to 1 for C₃S hydration at room temperature. Their fitting procedure and the quality of their fits were not described in enough detail to draw any firm conclusions regarding the large discrepancy in the magnitude of *m*. However, it should be noted that QXRD is not a particularly accurate technique for measuring the degree of hydration at early times.

Berliner et al.²¹ used quasielastic neutron scattering (QENS), a technique which measures the fraction of water which has become chemically bound, to measure the degree of hydration of C₃S at room temperature, using a few different *w/s*. Using the three-parameter Avrami model (eq 2), they report *m* values close to 2 for all *w/s*.

FitzGerald et al.⁹ also used QENS to measure the early hydration kinetics of C₃S at four different temperatures. Their data have significantly higher resolution than the data of Berliner et al.,²¹ and they used the four-parameter Avrami model to model the early rate of hydration. They were able to fit the data from the main hydration peak quite accurately, resulting in *m* values which increased from 2.15 to 2.59 as the hydration temperature increased from 20 to 40 °C. Their reported Avrami fit parameters are listed in Table 5. Because of the apparent quality of their data fits, this variation appears to indicate a true change in *m* with temperature.

One important difference with the current study is that FitzGerald et al.⁹ were able to fit the experimental kinetic data to a point where the rate dropped to ~10% of the maximum in the hydration rate, while, as stated earlier, fits to the current results could only be continued until the rate dropped to ~70% of its maximum value (see Figure 3). FitzGerald et al.⁹ performed one isothermal calorimetry run at 20 °C and overlaid the rate curve with their QENS results. There is a divergence of the curves on the downslope of the main

Table 6. Comparison between the True Activation Energy Calculated from the Rate Constants and the Apparent Activation Energy for the Time to Reach the Maximum Hydration Rate

paste	<i>E</i> _a (kJ/mol)	
	from rate constants	from <i>t</i> _{max}
C ₃ S/H ₂ O, no mix	35.2	32.4
C ₃ S/H ₂ O, 5-min mix	36.3	36.0
C ₃ S/D ₂ O, no mix	38.1	36.8
C ₃ S/D ₂ O, 5-min mix	39.4	41.0
FitzGerald et al. ⁹	36.8	34.6

hydration peak, with their calorimetry data more closely matching the current results. This suggests that there is a qualitative difference in the data obtained from thermal calorimetry and QENS.

If the value of the Avrami nucleation and growth exponent changes with temperature, this will affect the shape of the hydration rate curves. For example, the theoretical time to reach the peak in the reaction rate can be calculated from eq 3 as

$$t_{\max} = t_0 + \left(\frac{m-1}{m}\right)^{1/m} \frac{1}{k} \quad (7)$$

For given values of the rate constant and *t*₀, *t*_{max} will decrease as *m* increases and vice versa. Since the values of *t*_{max} and *t*₀ can be determined directly from the experimental data without resorting to a fit, this provides a way to determine independently whether the value of *m* changes with temperature. Equation 7 can be rearranged to give

$$\ln(t_{\max} - t_0) = -\ln\left[\left(\frac{m}{m-1}\right)^{1/m} k\right] \quad (8)$$

By plotting ln(*t*_{max} - *t*₀) vs 1/*T*, an apparent activation energy for the temperature dependence of the time to the peak hydration rate can be obtained. From eq 8, it can be seen that if the value of *m* does not change with temperature, then this apparent activation energy should be equal to the true activation energy calculated from the rate constants. However, if *m* increases with temperature the apparent activation energy will be lower than *E*_a, and vice versa.

Table 6 lists the apparent activation energies for the time to the peak hydration rate, along with the true activation energies. The Arrhenius fits in this case were not as linear as the ones shown in Figure 4. However, the values are quite similar for each type of paste, suggesting that the Avrami exponent does not change significantly with temperature for the current results. For the increase in *m* with temperature reported by FitzGerald et al.,⁹ eq 8 would predict that the apparent activation energy would decrease slightly from the true value of 36.8 kJ/mol to ~33 kJ/mol. This is in reasonably good agreement with the measured apparent activation energy of 34.6 kJ/mol (see Table 6). Therefore, according to this analysis neither the increase in the Avrami exponent with temperature measured by FitzGerald et al. using QENS nor the constant exponent measured in this work using calorimetry can be ruled out.

Using eq 4, it is possible to relate the Avrami exponent to three additional parameters, which describe the time dependence of the nucleation and growth process. For a value of *m* near 2.5, there are a few

(20) Double, D. D.; Hellowell, A.; Perry, S. J. *Proc. R. Soc. London A* **1978**, *359*, 435.

(21) Berliner, R.; Popovici, M.; Herwig, K. W.; Berliner, M.; Jennings, H. M.; Thomas, J. J. *Cem. Concr. Res.* **1998**, *28*, 231.

different combinations of P , S , and Q that are possible. One reasonable choice would be $S = 1$, indicating interface- or phase boundary-controlled growth, $Q = 0$, indicating zero nucleation rate, and $P = 2.5$, indicating an average product morphology between platelike (2D) and polygonal (3D). It is important to note that due to the lack of independent information concerning the details of C_3S hydration, almost any value of m less than 4 can be justified with these three parameters. For example, Brown et al.⁸ justified an m value of 1 by noting microscopic evidence for one-dimensional growth of C-S-H ($P = 1$).

Effect of D_2O on the Hydration Kinetics. Pastes hydrated with D_2O had a longer induction period and smaller rate constant than pastes hydrated with H_2O , but there was no significant difference in the Avrami exponents (see Table 2). The ratio of the H_2O rate constant to the D_2O rate constant decreases slightly with temperature, from 3.0 at 20 °C to 2.8 at 40 °C, and this is reflected in the higher activation energies for C_3S/D_2O pastes (see Table 4). These results are in good agreement with the results of King et al.,⁶ who performed isothermal calorimetry at 25 °C and noted that the plot of the rate of heat output vs time for the C_3S/H_2O paste could be closely reproduced by multiplying the time component of the C_3S/D_2O heat output data by a factor of ~ 2.7 .

King et al.⁶ noted the lower solubility of most salts in D_2O and suggested that the difference in the reaction rates is the result of a slower rate of dissolution of C_3S into D_2O and that as a necessary consequence the rate of C_3S dissolution is the rate-controlling step in the early hydration reaction. However, such a rate-controlling step is not consistent with an accelerating rate of reaction,⁴ and this explanation seems unsatisfactory in light of the extremely high solubility of C_3S .

It seems much more likely that the rate-controlling step is the rate of chemical reaction between ionic species in solution and that the observed reduction in the hydration kinetics for C_3S/D_2O pastes is a kinetic isotope effect. When an atom in a reactant molecule is replaced by a heavier isotope, the equilibrium constant for that reaction is lowered, and the rate of reaction is slowed. These changes, called isotope effects, are due solely to the change in atomic mass, and the magnitude of the effect depends on the relative sizes of the isotopes.¹¹ The greatest isotope effects occur when a hydrogen atom is replaced by deuterium (D) or tritium (T), which doubles or triples the atomic mass.

A general theory of isotope effects was developed by Urey²² and Bigeleisen and Mayer,²³ and Bigeleisen²⁴ was the first to treat kinetic isotope effects on the basis of conventional transition-state theory. A good general treatment of isotope effects can be found in the text by Laidler,¹¹ and the following simplified discussion is taken from there.

The magnitude of the isotope effect is always larger when the substituted isotope is part of a bond that is broken or formed during the rate-controlling step of the reaction, and when this is the case the effect is referred to as primary. If the substituted isotope is not directly

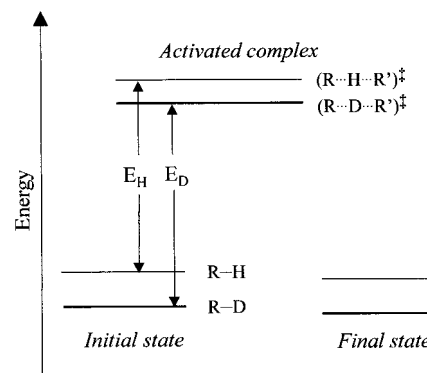
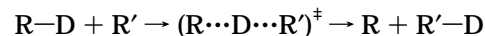
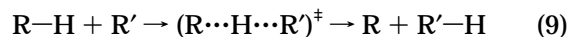


Figure 5. Schematic of the potential energy profile for the idealized reactions given by eq 9 (after Laidler¹¹).

involved in the reaction, the change in the kinetics is generally orders of magnitude smaller, and the effect is referred to as secondary. Measurements of isotope effects are sometimes used to elucidate information about a particular chemical reaction, particularly for determining whether a particular bond is involved in the rate-controlling step of a reaction.

A chemical reaction involving the breaking and reforming of a bond with a hydrogen or deuterium atom can be written as



where R and R' are any radicals. Following conventional transition state theory, the middle terms in parentheses are high-energy activated complexes. It is useful to envision the energetics of these reactions in terms of a potential energy surface, as shown in Figure 5. The initial state lies in the potential well toward the left, and the reaction is completed by moving to the right over the potential barrier, which requires forming a high-energy activated complex.

The replacement of H with D does not change the shape of the potential energy surface. However, it does change the zero-point energy of the molecules. Near room temperature most atoms are at or near their zero-point energy, represented by the lines $R-H$ and $R-D$ in Figure 5. The zero-point energy of the $R-D$ bond is lower than the zero-point energy of $R-H$, due to the larger mass of the deuterium atom.

The energies required to form the activated complexes are E_H and E_D . These energies are closely related to the activation energy for the reaction, E_a . As illustrated by Figure 5, the difference in the zero-point energies of the activated complexes $(R \cdots D \cdots R')^\ddagger$ and $(R \cdots H \cdots R')^\ddagger$ is always less than the difference in zero-point energies of the starting molecules. Therefore, the overall difference in energies for this reaction, $E_D - E_H$, is always positive, and the rate of reaction will be lower for D than for H. The relative reaction rates can be written as

$$\frac{k_H}{k_D} = \frac{A_H}{A_D} \exp\left(\frac{E_D - E_H}{RT}\right) \quad (10)$$

where A is the Arrhenius preexponential factor. For primary kinetic isotope effects, the ratio A_H/A_D is almost always between 0.7 and 1.4, and is usually quite close

(22) Urey, H. C. *J. Chem. Phys.* **1947**, *15*, 569.

(23) Bigeleisen, J.; Mayer, M. G. *J. Chem. Phys.* **1947**, *15*, 261.

(24) Bigeleisen, J. *J. Chem. Phys.* **1947**, *17*, 675.

to 1.²⁵ Equation 10 therefore predicts that the difference in activation energies for the reactions involving D and H will be related to the difference in reaction rates.

Using the values given in Table 4, the difference in activation energies for the early hydration of C₃S can be estimated as being 2.9–3.1 kJ/mol. Using the average value of 3 kJ/mol, and assuming $A_H/A_D = 1$, this would imply a ratio of reaction rates of 3.17 at 40 °C and 3.42 at 20 °C. These values are in quite reasonable agreement with the observed range of 2.78–3.02.

Conclusions

The rate of heat evolution during the period of fast hydration of C₃S pastes made with both H₂O and D₂O was accurately modeled using a four-parameter Avrami nucleation and growth equation. The kinetic data were fitted from the time of initial mixing to a time past the maximum in the rate of heat evolution. The Avrami exponent m , which is related to the morphology of the product phase, was found to be relatively constant for all pastes, with an average value of about 2.6.

Rapid hand mixing of C₃S pastes caused a decrease in both the time to reach the heat evolution peak (t_{\max}) and in the magnitude of the peak (R_{\max}), as compared to pastes which underwent only minimal mixing. For a given mixing condition, data for R_{\max} vs t_{\max} at different

temperatures and with H₂O and D₂O could be fitted using a simple inverse proportionality.

The reaction between C₃S and D₂O was found to be slower than the reaction with H₂O, in agreement with previous findings. The ratio of the nucleation and growth rate constants for pastes made with H₂O and D₂O ranged from 3.02 at 20 °C to 2.78 at 40 °C.

A survey of reported activation energies for the early hydration kinetics indicates that almost all values fall between 30 and 41 kJ/mol. The activation energies calculated in this work were 35–36 kJ/mol for C₃S/H₂O and 38–39 kJ/mol for C₃S/D₂O pastes.

Both the slower reaction rate and the higher activation energy of C₃S/D₂O pastes can be explained by a primary kinetic isotope effect. This indicates that the rate-controlling step in the early hydration reaction is the rate of a chemical reaction step that involves the breaking of a bond involving a hydrogen atom.

Acknowledgment. We thank Andrew Allen at the National Institute of Standards and Technology for useful discussions and for first bringing to our attention the increased time to set of cement pastes hydrated with D₂O. Financial support from the U.S. Department of Energy, Office of Basic Energy Sciences, under grant number DE-FG02-91ER45460 is gratefully acknowledged.

CM9900857

(25) Schneider, M. E.; Stern, M. J. *J. Am. Chem. Soc.* **1972**, *94*, 1517.